Refill Friction Stir Spot Weld Repair of a Fatigue Crack

Prepared by:

Sean Long Fox

Undergraduate, Metallurgical Engineering

Faculty Advisors:

Dr. Michael West

REU Site Director, Department of Materials and Metallurgical Engineering

Dr. Bahrat Jasthi

Research Associate, SDSMT Advanced Materials Processing Center

Dr. Alfred Boysen

Professor, Department of Humanities

Program Information:

National Science Foundation

Grant #: 0852057

Research Experience for Undergraduates

Summer 2010

South Dakota School of Mines and Technology

501 E Saint Joseph Street

Rapid City, SD 57701

TABLE OF CONTENTS

ABSTRACT

The main objective of this project is to repair a fatigue crack using Refill Friction Stir Spot Weld Technology. This involved developing a procedure to stitch, or overlap, single spot weld to repair fatigue cracks. A pre-cracking procedure was also developed to provide simulated fatigue cracks on which repairs could be made. First, the welding parameters were optimized for 2024 Al T3 with a thickness of .125 inches. 2024 powder is then deposited using Cold Spray Deposition to fill the pre-crack. The welds were then overlapped and repairs were made. The repairs were found to have defects and the defects are characterized to show how they reduced fatigue life. Good repairs are also characterized and show improvement in fatigue life over cracked samples. Improved repair methods are discussed to allow for better repairs in the future.

INTRODUCTION

Fatigue life is a very important factor in many applications. For instance, a plane wing will undergo fatigue cycles as the wing flutters during flight. Over time this cyclic fatigue will cause fatigue cracks. With every cycle, the fatigue crack grows larger. Many times these fatigue cracks act as an indicator that the part in question must be replaced. These replacements are costly and require constant manufacturing. Recently, a new friction stir process was developed called Refill Friction Spot Welding. With this new idea, Harms and Wende of Germany has developed a small RFSW machine. The RFSW process differs from traditional friction spot welding. The friction stir refill process uses a pin and sleeve (shoulder) that move independently from each other. While both pin and sleeve are rotating, the sleeve is plunged into the material to be welded. At the same time, the pin retracts upward; drawing plasticized material up as well. Once the sleeve has reached its full depth, both sleeve and pin return to their original position. As the pin moves down, it re-introduces the plasticized material back into the weld. This method of friction stir spot welding has been shown to be superior to the fixed pin of friction spot welding. Using the RFSW process, a procedure for repairing existing fatigue cracks could be developed. Repairing a part can be much more cost effective when compared with simply replacing the part. It is with this goal in mind that a procedure for RFSW fatigue crack repair will be developed.

In order to repair a fatigue crack, it must first be created in a sample that can be analyzed. 2024 Aluminum in a T3 state will be used as the material to be tested. A thickness of 0.125 inches will be used as it is a common size for many Al skin applications. This thickness is also near the limit of the RFSW machine’s welding depth. A sample configuration was selected as per ASTM E647 for a notched sample. The specimen is a dog bone configuration. The samples are then machined under high tolerances and a pre-crack is introduced into the test cross section. The pre-crack acts as a stress concentrator and helps to grow the fatigue crack. The crack will be grown under cyclic loading condition in a MTS 810 tensile testing machine. Once a fatigue crack is present, the pre-crack volume loss must then be filled to allow for proper surfacing during RFSW repair. For this a Cold Spray Process will be used to introduce 2024 Al powder into the pre-crack. Then, stitch welds will be used to repair the fatigue crack that remains in the sample. A stitch weld is simply overlapping welds to form a continuous repair. Once repaired, the sample will then undergo addition fatigue test to show the resulting fatigue life. This is then compared to the fatigue life of parent metal samples and to that of unrepaired samples. The un-repaired samples simply have the unrepaired fatigue crack present. Ultimately this will show whether the procedure outlined in this project will give an improved fatigue life for this material.

BROADER IMPACT

In order for a part to develop a fatigue crack the part simply must undergo cyclic stress at a level below the materials flow stress. The crack will generally form near a stress concentrator. Sharp ninety degree angles, or areas of weakness, make good stress concentrators. Once the crack is started it will spread to a point when the part may fail in a catastrophic manner. Replacement parts are costly and they rely on their supply. One good example of how fatigue cracks can be harmful would be the United States Military’s aging equipment. For instance, the F-15 eagle is an aircraft that has been around since the early 1970’s. As this aircraft flies through the air, the tips of the wings flutter up and down. This causes fatigue cracks to form in the wing. A replacement wing is a costly option, but what if it could be effectively repaired? Time, money, and resources could be saved with an effective repair procedure. Solution such as this are needed to caring aging equipment into the future without having to maintain the associated infrastructure. This means that a piece of machinery could still be used even without parts being actively manufactured. The military example is not where the possibilities end. The private sector could also benefit much from an effective fatigue crack repair process.

PROCEDURE

Materials Preparation

The materials that were used in this project were 2024 Aluminum in the T3 state. The 2024 Aluminum plate was 0.125 inches thick. Originally, this material was a single plate. This plate was then sheered to a dimension with approximated 0.125 inches excess in each dimension. It should be noted that the length (12in) of the specimen is the original direction of rolling. The raw sheered plates where then squared to within .1 inches of their final dimensions. This was done using a manual milling machine, with great care taken to achieve high tolerances. Instead of the traditional 0.02 inches tolerances, 0.01 inches was selected. Precisely machined samples are needed to ensure good results. ASTM E466 was the standard referred to while finalizing the sample configuration. The rectangular plates then needed some final milling to introduce the reduced section. This milling was performed using a CNC milling machine. The radius of the reduced section was 0.5 inches. The final pass in the CNC was a high tolerance and surfacing pass. This means that only 0.005 inches were removed on the last pass in order to maintain the high tolerance. The samples were stacked 8 high or 1 inch thick for the CNC milling process. Figure 1 illustrates the final specimen and the location of the pre-crack, while Figure 2 shows the Solidworks model used to develop the tool paths for final CNC milling.

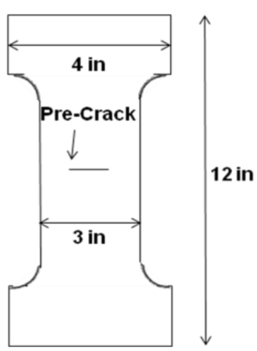

Figure1: Sample Configuration

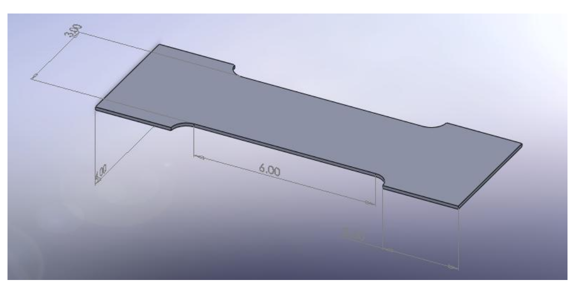

Figure 2: Solidworks Coupon Model

Pre-Cracking and Fatigue Crack Growth

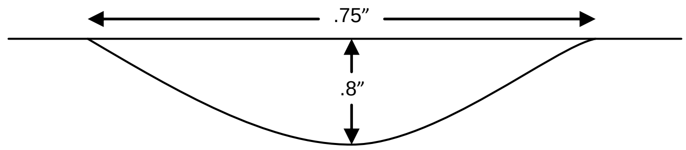

The pre-crack growth procedure was setup using a Dremel power tool. The tool had a 1/8 inch thick disk made of silicon carbide. The procedure was to cut a .80 inch deep and .75 inch long slot out of the fatigue coupon to initiate a fatigue crack growth.

Figure 3: Pre-Crack Dimension (front)

Figure 3 shows the diagram and shows the dimensions of the pre-crack.

This was the first step in artificially creating a fatigue crack. After the pre-crack was initiated the coupon was then loaded into a tensile test machine. The coupons were run in cyclic fatigue to broaden the width and depth of the fatigue crack. The range for the load of the cyclic fatigue was from .675 kips to 6.75 kips. The 6.75 kips is thirty percent of the flow stress of the material. The range of the load needed to be low to ensure a plastic region did not form around the crack. The test were performed at 20 Hz and reached approximately 50,000 cycles. Figure 4 shows a close look on a finished fatigue crack. It can be seen that the pre-crack dominates the visual; however there are microscopic cracks on each side of the pre-crack. The total width of the crack was approximately .78 inches to .65 inches. A closer look at this macroscopically indicates that indeed a crack was propagated in the pre-crack. In Figure 5, it shows the crack at a 50x resolution.

Figure 4: Fatigue Crack Width

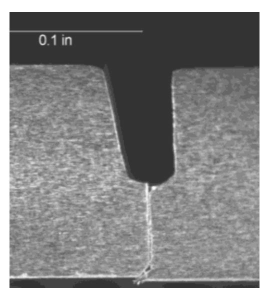

Figure 5: Fatigue Crack Macro (side)

Fatigue Test

The cyclic fatigues of the samples are broken up into three categories. The categories consist of parent, un-repaired and repaired samples. Each category will have 4 load levels applied to them. The are expressed as percentage of flow stress. The load levels include 20% at .45 kips to 4.5 kips, 30% at .675 to 6.75 kips, 40% at .9 kips to 9.0 kips and 50% at 1.125 kips to 11.25 kips. Making the total flow stress for the coupon to be 22.5 kips. These are the cyclic fatigues lower and upper limits and will proceed until failure of the material is reached. In Figure 6, an unrepaired sample that was run until failure is shown.

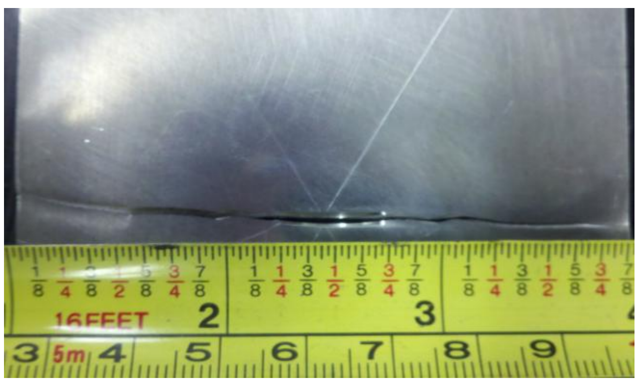

Figure 6: Failure of an Un-Repaired Sample

Optimization of Parameters

For the welding part of the project, optimized parameters are needed. Previous work was done using this exact procedure of optimization, however, the state of RFSW machine was unsteady at that time. A parameter matrix was developed and can be seen below in Figure 7. In order to show the best combination of weld time and rotational speed, each must be varied to show the overall affect on weld defects. By increasing these variables an increase in the mixing and heat input may be seen. In order to see the best combination, 1400 to 1600 rpm was tested, with the total weld time varying from 6 to 10 seconds. It should be noted that the total weld time includes the plunge time and the retraction time. In this experiment the plunge time is equal to the retraction time. The clamping pressure is constant at 3.5 bar. Clamping pressure is applied through a standard pneumatic c-gun which forms the frame of the RFSW. The clamp, or gun, is actuated at the beginning of the welding cycle and lifts the material up to the clamping ring, which contains the sleeve and pin. Additional clamping is applied to the front and the back of the plate in the form of secured blocks. This prevents the coupon from rotating during the welding process. After the welds were made for the parameter matrix, the samples were polished down to a one micron diamond polish and then etched with Kellar's.

The parameter matrix in Figure 7 shows the results of the parameter development process. The sections marked no weld are the result of the machine retaining most of the material that was plasticized. This resulted in a large hole in the aluminum plate. This most certainly indicates unacceptable parameters. Early in the parameter investigation, parameters were explored below the range shown in the chart with a particularly bad result, current limits were triggered. This means that the force required to rotate the tools required an amount of current outside the operational range of the RFSW machine. The parameters expressed on the chart are the lowest within the operation range of the machine. This tells us that with bad welds at higher variable levels and force limits on the low end of the matrix, an optimized parameter should be within the matrix. Another consideration in the welding procedure is the surfacing. An addition welding step was added at the end of the welding process in order to give the best surfacing possible. This was kept constant as a 1 mm plunge, 1 sec total weld time, and 1400 rpm plunge. As a result, the material along the surface is returned to the 2024 aluminum plate and a nearly flush surface is achieved. This surfacing step will be discussed in further detail.

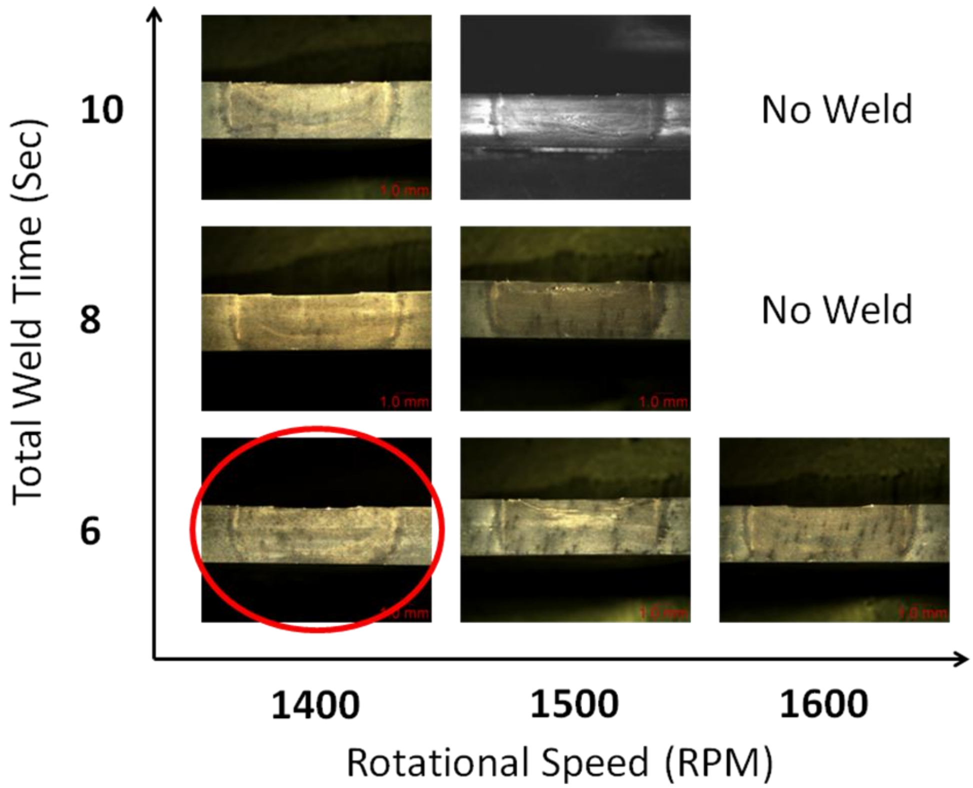

Figure 7: Developmental Matrix

Within the matrix, observations were made to show the best set of parameters. The criterion of a good weld involves observation of the formation of defects. In the 1500 rpm set of samples, a lack of mixing near the surface can be seen. In 1500 rpm sample, the six and eight second welds show voiding near the surface as a result of the lack of mixing. These features can very easily initiate fatigue cracks and thus are seen as un-acceptable welds. Another consideration is the mixing along the walls of the weld. A thin light colored line can be seen in all welds along the left and right sides of each weld. This feature is caused by the sleeve plunging into the plate. The 1400 rpm, 6 second sample shows the best mixing in the walls of the weld. Using these observations, it was decided that the 1400 rpm, 6 second weld, is the most optimized parameter. Once again it is important to keep in mind that at variable levels below this yield no welds due to machine limits.

Surfacing and Penetration

Beyond the variation of RPM and Time, there are two other major factors in showing a good weld from a fatigue standpoint: penetration and surfacing. When it comes to penetration, this machine is at its limit with 3.175 mm (0.125 inch) thick material. Luckily the area under the pin is stirred and a full depth plunge is not necessary. As a result, the plunge depth for all welds is 2.8 mm. As seen in the parameter matrix, all welds were stirred all the way to the bottom surface. This is important because the fatigue crack to be repaired extends through entire thickness of the plate. The other major factor left to discuss is surfacing. Right angles and indentations along the surface may be initiation sites for fatigue cracks, so the surface must be as flush as possible. This is accomplished by ensuring that there has been no volume loss from the fatigue cracking process, and by having a proper home position for the pin and sleeve. The volume loss is addressed by filling the pre-crack using a cold spray process. This process will be discussed in greater detail later. The home position is set by having the proper pin, sleeve, and clamping ring alignment. When the part is clamped, it is pressed upwards against the downward facing clamping ring. Within the clamping ring is the sleeve and pin. The bottom surface of these three components must be aligned when the tool is first installed into the machine. Further adjustments can be made after twenty conditioning welds using identical material. These conditioning welds fill the tool with aluminum, and prevent additional volume loss. Once the surface is as flush as possible the tool is ready to make repairs.

Stitch Welding

A single weld will not repair the entire fatigue crack. In order to stir the entire length of the crack, single spot welds must be overlapped into what is referred to as a stitch weld. In the previous year's study it was found that tensile strength varies with varying overlaps. Using digital image correlation to illustrate stress distribution around each configuration of stitch weld and the hardness across each configuration, an optimized stitch weld was found. It was shown that overlapping 4 welds by 0.216 inches, centered about the center of the fatigue crack, would give the best properties. This study was a comparison of configurations with identical weld conditions so this study is used for this project as well.

Cold Spray

Cold spray deposition will be used to fill the pre-crack that was created to grow the fatigue cracks. It is critical to make up for the volume loss, or else risk creating a fatigue initiation point along the surface. The cold spray process involves injecting a particle into a stream of gas and impacting the particle onto a substrate. The idea is that the particle needs enough energy to plasticize and bond with the surfacing. Energy is transferred from the gas to the particle as it accelerates within a nozzle. Generally the nozzle with involve converging and diverging chambers. The gas is also heated to allow for higher velocities. A cold spray deposition trial can be seen in Figure 8.

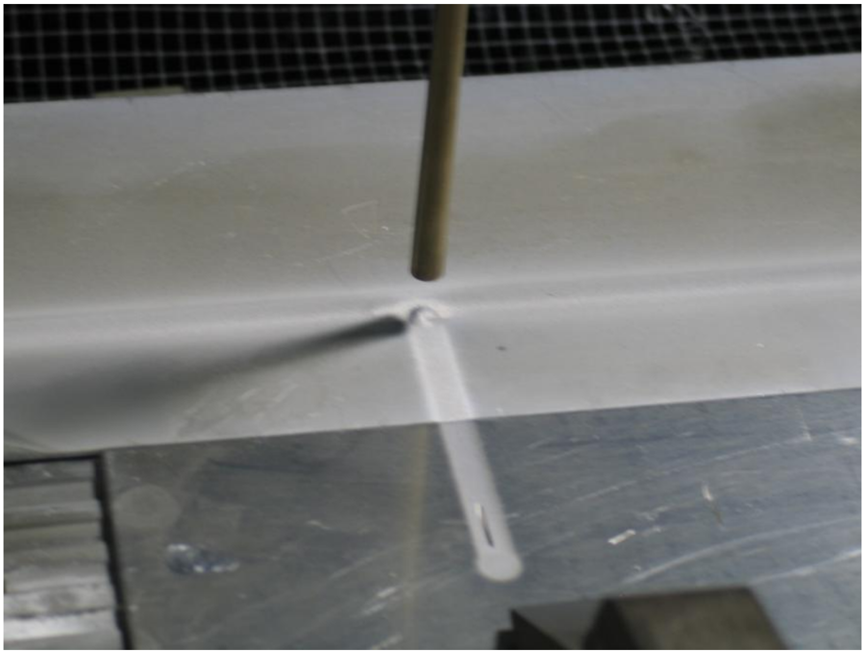

Figure 8: Cold Spray Deposition Trial with 2024 Al Powder (400 mesh)

Abdulaziz Alhulaifi is currently preparing a dissertation on the subject. With Abdulaziz's, work we have a better understanding of the process. The critical velocity can be calculated using Equation 1. This equation is the result of the energy balance. Note that the melting point for the material, 2024 Al in this case, is reduced by 30%. This is because only 70% of the melting temperature is needed for plasticization. The C_p and T_m come from Al 2024 known properties. The T_i is the temperature of the gas. The gas is generally heat between 250°C and 450°C. The gas can be varied, but compressed air between 80psi and 140psi has been the gas of choice up to this point. Using this equation the critical velocity for the 2024 Al powder was found to be 590 m/s. Additionally, the size of the sprayed particle is crucial for achieving a deposit. The 2024 Al powder begins as 140 mesh, which means 105 microns is the largest size particle.

$$V_{critical} = \sqrt{C_p(.7T_m - T_i)}$$

Equation 1: Critical Velocity

After attempting for spray the 105 micron size material, it was found that no particles were sticking to the substrate. The variables were explored in depth with no positive result. In order to overcome this, the powder was sieved to reduce the size of particle sprayed. 44 micron and 37 micron particles were sieved. The pressure of the compressed air was varied from 80 psi to 140 psi and the temperature of the gas from 250^{o}C to 450^{o}C with only minimal deposition. The pressure is limited by the range that the lab air compressor can operate in. The deposition occurred with the 37 micron particle at max pressure and temperature. Loss was very large as few particles actually deposited. The possibility of strain hardened particles was explored. First, a polished sample was examined for geometry. This can be seen in Figure 9 below. Cleary the Al powder particles are small spheres, most likely from being atomized. Meaning it is less likely that they are strain hardened. Second, a micro hardness test was needed. A sample was prepared in an epoxy mount. This sample was then tested for Vicker's hardness. After 20 points were tested it was found that the average hardness was about 125 on the Vicker's scale. This is within 10 of the known 2024 Al hardness value, thus it was confirmed that no strain hardening occurred. After consulting Abdulaziz, he calculated that the system was not reaching the critical velocity and adjustments would be needed.

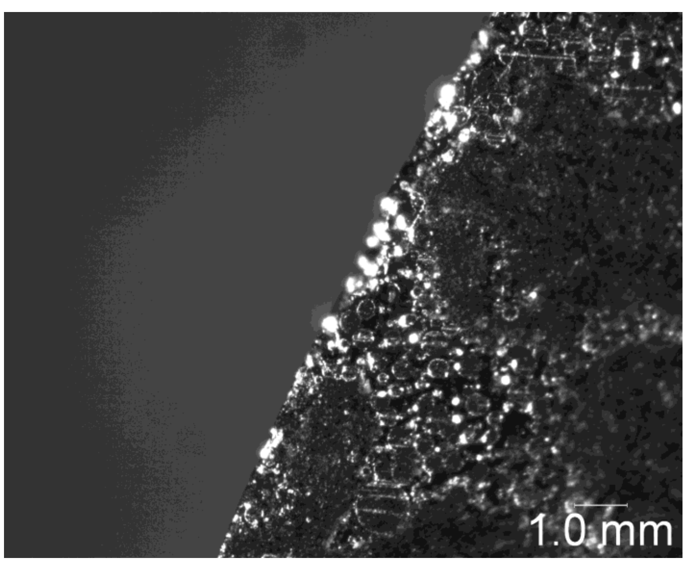

Figure 9: 2024 Al Powder in Bakelite at 2.5x

RESULTS

The cold spray process has not yet yielded a deposition. As a result, the final repairs have not yet been made. The fatigue testing of the parent material has been complete and can be seen in Figure 10. These values form the basis of a comparison with repaired and unrepaired samples.

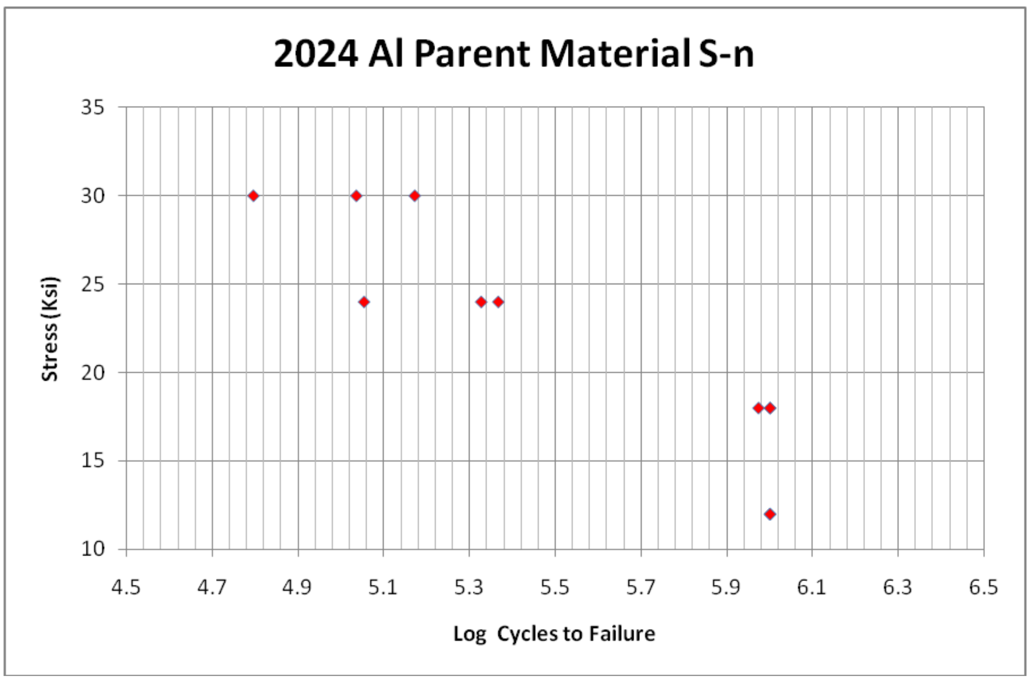

Figure 10: 2024 Al Parent Metal Fatigue Results

CONCLUSION/DISCUSSION

Future Work

Cold spray deposition and final repairs have yet to be completed. The cold spray deposition will require further investigation. In order to achieve this deposition, one of two methods will be used. One method involves depositing pure aluminum into the pre-crack. This method would involve a tertiary study on the effect of the pure aluminum addition on the properties of the resulting RFSW. If found the improve properties (tensile and fatigue), or if the properties remain unchanged, the method will be used for final repair. The second method for 2024 Al cold spray deposition involves further investigation into depositing the 2024 Al powder. Using the data from the previous attempts to deposit this material, we know that we must achieve a higher velocity. This may be achieved by one of several ways. First, the cold spray nozzle could be extended. This will give the particles more time to accelerate to the critical velocity. Another way this may be accomplished is simply by changing the distance from the end of the nozzle to the substrate from 13mm to 20mm. This may have a similar effect to the longer nozzle solution. Lastly, the gas used in the cold spray deposition process could be changed. Regardless of the gas chosen, the high pressure tanks that are delivered can provide much higher pressure than 140 psi. This may allow us to achieve double the pressure previously used. The gas may also be varied. Helium, and possibly nitrogen, may be used to propel the aluminum particles as well. The density of the helium gas may allow for higher impact velocities. The nitrogen gas will behave in a similar manner to the compressed air, but serve as a higher pressure source. Once the cold spray deposition process is finalized, final repair and testing can begin.

REFERENCES

Russel, SG. 2001. Static, Fatigue and Crack Growth Behavior of FSW 7075 T-6 and 2024 T-3 Aluminum Alloys. TMS Friction Stir Welding and Processing, Vol. 1, Pg 93

Oberembt, Clark. 2008 Effects of Process and Parameters on Joint Properties of Refill Friction Stir Spot Welded Magnesium-Aluminum Alloy. SDSMT Thesis.

Alhulaifi, Abdulaziz. 2009. Cold Spray Modeling for Spraying Nano Particle Powders. SDSMT Research Proposal.

Uematsu and Tokaji. 2008. Effect of Re-filling Probe Hole on Tensile Failure and Fatigue Behaviour of Friction stir Spot Welded Joints in Al–Mg–Si Alloy. International Journal of Fatigue, Vol. 10-11, Pg 1956-1966.

Uemetsu, 2009. Comparison of Fatigue and Tensile Behaviour Between Resistance Spot Welds and Friction Spot Welds. Science and Technology of Welding and Joining. Vol 14, Pg 62.

Referenced ASTM Standards:

ASTM E647- Measuring Fatigue Cracks

ASTM E466- Fatigue Test Practices

ASTM E468- Reporting Fatigue Test Results